Mic60 exhibits a coordinated clustered distribution along and across yeast and mammalian mitochondria

Stefan Stoldt[a,1], Till Stephan[a,1], Daniel C. Jans[b,c], Christian Brüser[a], Felix Lange[a], Jan Keller-Findeisen[a], Dietmar Riedel[d], Stefan W. Hell[a,2], and Stefan Jakobs[a,b,2]

[a]Department of NanoBiophotonics, Max Planck Institute for Biophysical Chemistry, 37077 Göttingen, Germany; [b]Clinic of Neurology, University Medical Center Göttingen, 37075 Göttingen, Germany; [c]Science for Life Laboratory, Department of Applied Physics, Royal Institute of Technology, 171 65 Stockholm, Sweden; and [d]Laboratory of Electron Microscopy, Max Planck Institute for Biophysical Chemistry, 37077 Göttingen, Germany

Contributed by Stefan W. Hell, March 14, 2019 (sent for review November 29, 2018; reviewed by Bo Huang and Nikolaus Pfanner)

Mitochondria are tubular double-membrane organelles essential for eukaryotic life. They form extended networks and exhibit an intricate inner membrane architecture. The MICOS (mitochondrial contact site and cristae organizing system) complex, crucial for proper architecture of the mitochondrial inner membrane, is localized primarily at crista junctions. Harnessing superresolution fluorescence microscopy, we demonstrate that Mic60, a subunit of the MICOS complex, as well as several of its interaction partners are arranged into intricate patterns in human and yeast mitochondria, suggesting an ordered distribution of the crista junctions. We show that Mic60 forms clusters that are preferentially localized in the inner membrane at two opposing sides of the mitochondrial tubules so that they form extended opposing distribution bands. These Mic60 distribution bands can be twisted, resulting in a helical arrangement. Focused ion beam milling-scanning electron microscopy showed that in yeast the twisting of the opposing distribution bands is echoed by the folding of the inner membrane. We show that establishment of the Mic60 distribution bands is largely independent of the cristae morphology. We suggest that Mic60 is part of an extended multiprotein interaction network that scaffolds mitochondria.

mitochondria | MICOS | mitoskeleton | FIB-SEM | nanoscopy

Mitochondria, the "powerhouses" of the cell, are double-membrane organelles that often form highly dynamic loose networks of tubules that frequently undergo fusion and fission, thereby continually changing the appearance of the network (1–3). Mitochondria communicate with the nucleus (4) and are physically connected to other organelles by means of interorganellar tethering (5, 6). The highly convoluted mitochondrial inner membrane is surrounded by the smooth outer membrane and has three contiguous domains: the inner boundary membrane that parallels the outer membrane; crista membranes, invaginations of the inner membrane that differ in shape depending on the cell type and physiological conditions; and crista junctions, narrow tubules that connect the inner boundary membrane with the cristae membrane.

Mitochondria arose from the engulfment of a proteobacterium by a precursor of the modern eukaryotic cell (7). Most, if not all, bacterial cells contain at least one skeletal protein system, often referred to as the "prokaryotic cytoskeleton" (8, 9). These prokaryotic cytoskeletons are vital for several functions, including cell shape determination and cell division. However, while in eukaryotic cells the cytoskeleton is defined by constitutive components, such as actin, tubulin, and intermediate filaments, the term prokaryotic cytoskeleton is generally used in a broader sense, encompassing a variety of systems that form superstructures within the bacterial cells (8, 9). Surprisingly, given the intricate architecture of the mitochondria, a large scaffolding structure, or "mitoskeleton," has not yet been demonstrated.

The mitochondrial contact site and cristae organizing system (MICOS; previously also known as MINOS, MitOs, or MIB) (10) is a conserved ancient hetero-oligomeric protein complex localized primarily at the crista junctions. The depletion of MICOS subunits results in a disturbed inner membrane morphology and a decreased number of crista junctions (11–15). The MICOS core component, Mic60, interacts physically with numerous proteins in the mitochondrial inner and outer membrane, thereby forming contact sites (12, 13, 15–20).

An earlier study insightfully proposed that MICOS forms a filamentous structure within the inner membrane of budding yeast mitochondria (13). This study relied on genetic interactions and diffraction-limited fluorescence microscopy, providing an optical resolution in the size regimen of the organelle diameter. Here, using stimulated emission depletion (STED) nanoscopy and focused ion beam milling combined with scanning electron microscopy (FIB-SEM), we analyzed the localization of the MICOS complex in relation to the inner membrane architecture. We show that subunits of the yeast and human MICOS complex form distinct clusters that are intricately arranged within the mitochondrial inner membrane, often localized in opposing distribution bands that can adopt a helical arrangement. Our data support the idea that MICOS is part of a multiprotein interaction network that encompasses MICOS as well as additional proteins in the mitochondrial membranes and thereby scaffolds the mitochondrion. We suggest that this scaffold is the elusive mitoskeleton.

Significance

The intricate folding of the mitochondrial inner membrane is essential for the functioning of mitochondria as cellular powerhouses. The mitochondrial contact site and cristae organizing system (MICOS) complex is localized at the crista junctions and is key for the establishment of proper architecture of the mitochondrial inner membrane. Relying on optical nanoscopy and focused ion beam-scanning electron microscopy, we demonstrate that Mic60, a subunit of the MICOS complex, forms clusters distributed in two opposing distribution bands, which can be twisted to produce a helical arrangement of the cristae. Our findings suggest that the Mic60 clusters are physically coupled along and across the mitochondrial tubules. The visualization of these distributions bands opens the door to a microscopic investigation of the proteins that scaffold mitochondria.

Author contributions: S.S., T.S., and S.J. designed research; S.S., T.S., D.C.J., C.B., F.L., and D.R. performed research; J.K.-F. contributed new reagents/analytic tools; S.S., T.S., D.C.J., C.B., J.K.-F., S.W.H., and S.J. analyzed data; and S.S., T.S., and S.J. wrote the paper.

Reviewers: B.H., University of California, San Francisco; and N.P., University of Freiburg.

The authors declare no conflict of interest.

[1]S.S. and T.S. contributed equally to this work.

[2]To whom correspondence may be addressed. Email: stefan.hell@mpibpc.mpg.de or sjakobs@gwdg.de.

This article contains supporting information online at www.pnas.org/lookup/suppl/doi:10.1073/pnas.1820364116/-/DCSupplemental.

Published online April 26, 2019.

Results

Crista Junctions Are Frequently Arranged in a Helical Pattern in Budding Yeast Mitochondria. The MICOS core component Mic60 is an integral protein of the mitochondrial inner membrane required for the proper folding of this membrane (10, 11). To reevaluate the nanoscale distribution of Mic60 in the budding yeast *Saccharomyces cerevisiae*, we genomically tagged Mic60 with GFP and immunolabeled the cells with a GFP antibody, thereby carefully optimizing the labeling conditions. Because of the small diameter of the mitochondria, diffraction-limited confocal microscopy was insufficient to reveal details of the submitochondrial distribution of Mic60 (Fig. 1*A*). Using STED nanoscopy (21, 22), we found that Mic60 was frequently located in distinct clusters on two opposing sides of a mitochondrion, so that they appeared to be enriched in two opposing distribution bands that were running along the mitochondrial tubules (Fig. 1 *A* and *B* and *SI Appendix*, Fig. S1*A*). This clustered distribution could not be attributed to a fixation or imaging artifact, as STED recordings of yeast cells expressing matrix-targeted GFP showed a homogenous distribution of the fluorescence signal across the mitochondria with no indications of clusters (*SI Appendix*, Fig. S1*B*). In more than 45% of all cells (n = 303), sections of the Mic60 distribution bands appeared to be twisted, so that the arrangement of the Mic60 clusters was reminiscent of a helix.

As Mic60 is enriched at crista junctions (11, 12, 23), such a helical arrangement suggests that the crista junctions and also the cristae are preferentially arranged in a spiral pattern. To test this hypothesis, we performed FIB-SEM and created 3D reconstructions of the inner membrane architecture of the mitochondrial network of wild-type yeast cells (Fig. 1*C*, *SI Appendix*, Fig. S1 *C* and *D*, and Movie S1). The 3D reconstructions revealed that most cristae were rather sheet-like, and that almost none of them spanned the mitochondria from one side to the other. The generally rather short cristae were found mostly at two opposing sides of the mitochondrial tubule (*SI Appendix*, Fig. S1 *E*–*G*). In large parts of the mitochondria, a spiral-like arrangement of the cristae was visible (Fig. 1 *C* and *D*, *SI Appendix*, Fig. S1 *E*–*G*, and Movie S1). Intriguingly, the animated display of virtual consecutive transversal sections along a mitochondrion resulted in the impression of a propeller-like rotation of the cristae (Fig. 1 *D* and *E* and Movie S1). Even without 3D reconstructions, this rotation of the cristae was immediately visible in the majority (>80%) of all yeast cells within a FIB-SEM stack (Fig. 1*F*). Thus, the STED data and FIB-SEM recordings point to an ordered arrangement of Mic60, the cristae, and the crista junctions in yeast mitochondria.

Although we observed helical Mic60 patterns in approximately 45% (n = 303) of the yeast cells, a detailed quantification beyond the repeated observation of the helical arrangement of Mic60 clusters (*SI Appendix*, Fig. S1*A*) is very challenging in yeast, because this analysis is inevitably hampered by the strong bending of the mitochondrial tubules within the small spherical cells. Furthermore, immunolabeling of yeast cells for superresolution

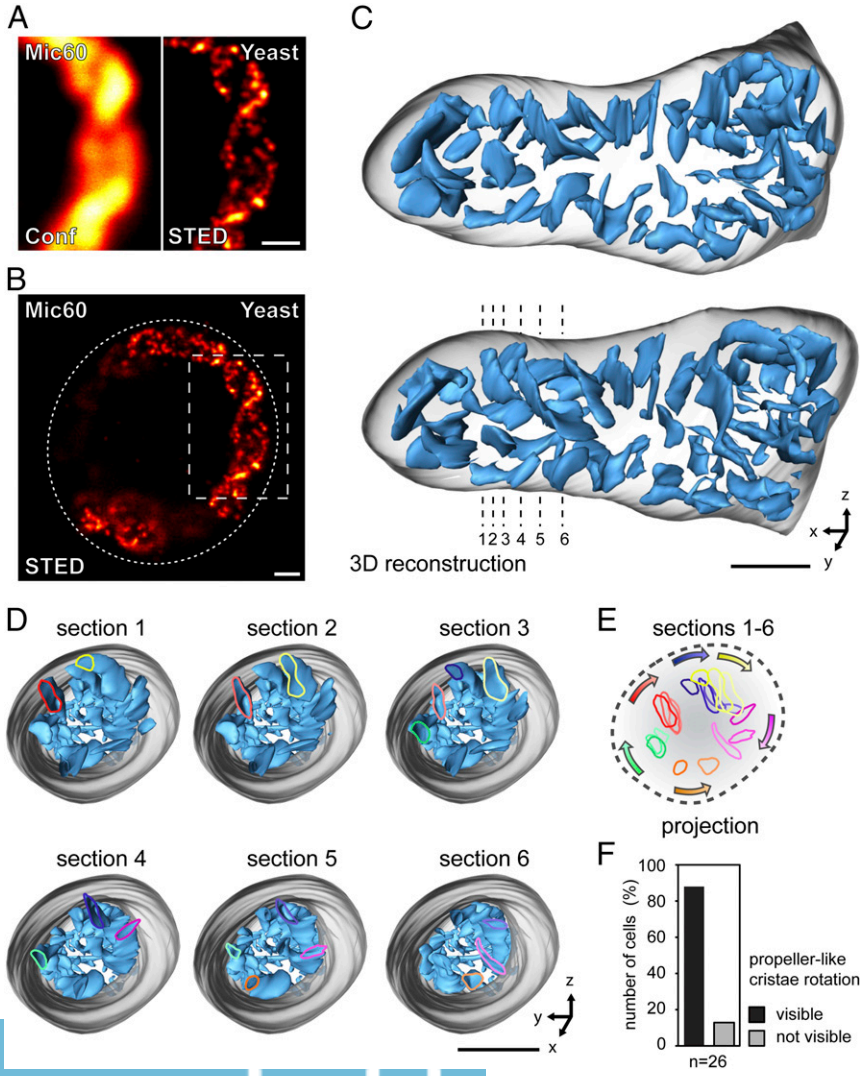

Fig. 1. Mic60 and the cristae are often arranged in a helical pattern in budding yeast mitochondria. (*A* and *B*) Submitochondrial localization of Mic60-GFP in budding yeast grown in galactose medium. Cells were labeled with a GFP-specific antiserum. (*A*) The comparison between confocal microscopy and STED nanoscopy demonstrates the resolution improvement achieved by STED nanoscopy. (*B*) 2D STED image of an entire yeast cell; the image shows the same cell as magnified in *A*, as indicated by a rectangle. (*C*) FIB-SEM recording of a budding yeast cell grown in galactose medium. Part of a reconstructed mitochondrion is shown. The cristae are rendered in blue; the outer membrane, in gray. Shown are two different views of the same mitochondrion. (*D*) Consecutive transversal cross-sections through the reconstructed mitochondrion at sites indicated in *C*. The contours of six cristae are highlighted with different colors to visualize the orientation of the cristae along the longitudinal axis of the mitochondrion. (*E*) Projections of the cristae contours shown in *C*. Colors fade with ascending section numbers. Arrows indicate the apparent rotation of the cristae. (*F*) Quantification of yeast cells showing twisted cristae arrangements, based on FIB-SEM recordings. (Scale bars: 400 nm in *A* and *B*; 150 nm in *C* and *D*.)

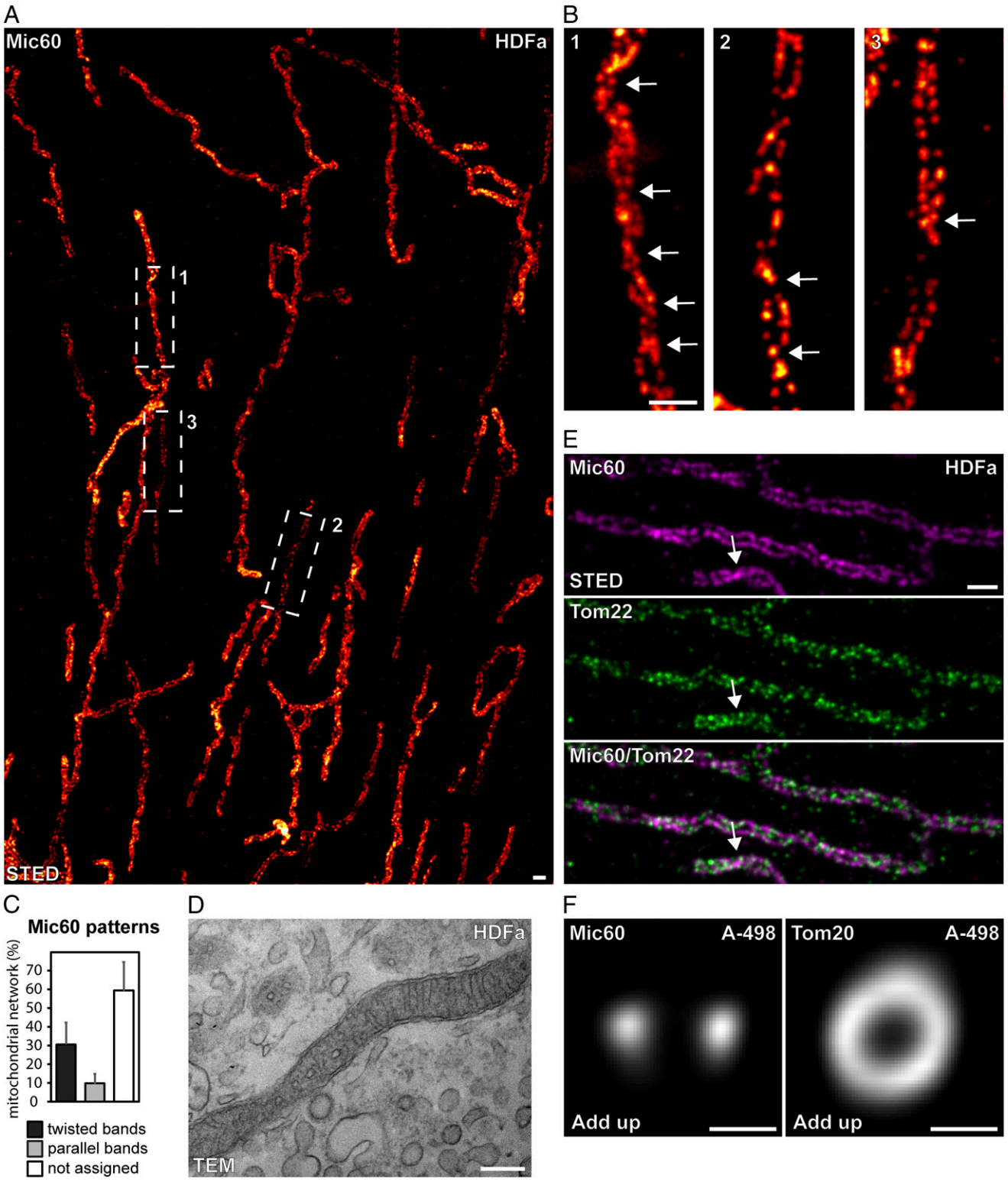

Fig. 2. Nanoscale distribution of Mic60 in human mitochondria. (*A*) STED nanoscopy of Mic60 in primary HDFa cells. (*B*) Magnifications of the areas indicated in *A*. Arrows indicate twisting sites. (*C*) Quantification of the frequency of occurrences of twisted or parallel Mic60 distribution bands in HDFa cells. For the analysis, parts of the mitochondrial networks of 18 HDFa cells, corresponding to ∼14-mm mitochondrial tubules, were manually assigned by three test persons to the different categories. Error bars represent SDs of the three independent analyses. (*D*) TEM image of a mitochondrion of an HDFa cell. (*E*) Dual-color STED image of an HDFa cell decorated for Mic60 and Tom22. The arrow points to a twisting site of the Mic60 distribution bands, whereas the outer membrane labeled by Tom22 is not constricted. (*F*) Longitudinal add ups of Mic60 and Tom20 fluorescence signals in mitochondria from human A-498 cells. The add ups cover 1.5-μm sections of the mitochondrial tubule. For Mic60, a tubule section with a parallel distribution of Mic60 clusters was selected. Shown are exemplary images; statistical analysis data are provided in *SI Appendix*, Fig. S3. For all images, Mic60, Tom22, and Tom20 were decorated with specific antisera. (Scale bars: 500 nm in *A*, *B*, and *E*; 200 nm in *C* and *F*.)

microscopy is technically demanding, resulting in numerous damaged cells, and thus requires a manual selection of the imaged cells.

A Helical Arrangement of Mic60 Clusters Is Also Frequent in Human Mitochondria. We next investigated whether the helical arrangement of the Mic60 clusters is a peculiarity of the highly curved yeast mitochondria or whether it can also be found in human mitochondria. We decorated adult human dermal fibroblasts (HDFa) with an antiserum against Mic60 and recorded them with 2D STED nanoscopy (Fig. 2 *A* and *B* and *SI Appendix*, Fig. S2*A*). As reported previously (23), the MICOS clusters were spaced regularly along the longitudinal axis of mitochondria and often appeared to be localized in two parallel distribution bands in the mitochondrial tubule. Manual assignment of large areas of the mitochondrial network revealed that in HDFa cells, these bands of clusters were parallel in approximately 10% of the mitochondrial network, while twists of the Mic60 distribution bands were observed in approximately 30% of the mitochondrial network (Fig. 2*C* and *SI Appendix*, Fig. S2*A*). The remaining ∼60% of the network was not clearly assignable to one type of pattern, because of either partially out-of-focus mitochondria or an excessively high density of Mic60 clusters. Possibly the distribution bands were also wider in these cases, so that they were no longer clearly discernible. Parallel and helical arrangements of Mic60 distribution bands were found in the same cell, often in immediate proximity (Fig. 2 *A* and *B* and *SI Appendix*, Fig. S2*A*), demonstrating that the twisted arrangement is not restricted to curved mitochondria.

To investigate the mean distance between the individual Mic60 clusters, we used a computer algorithm to straighten in silico 91 mitochondrial tubules from 13 fibroblasts (*SI Appendix*, Fig. S2*B*). The mean distance between neighboring clusters within one distribution band along the longitudinal axis of the mitochondria was 135 ± 72 nm (*SI Appendix*, Fig. S2 *B* and *C*). The clusters in one distribution band seemed to be spatially correlated with the clusters in the opposing band. To quantify this observation, we determined the correlation of the Mic60 signal of directly opposing sides in the straightened mitochondria. The Pearson correlation coefficient was 0.39 between the two bands. When one of the distribution bands was shifted in silico with respect to the other by >500 nm, the Pearson correlation coefficient was almost 0, which indicates no correlation. From this, we conclude that compared with a random scenario, that Mic60 clusters often appear in opposing pairs.

Using transmission EM (TEM), we next analyzed the cristae architecture in these primary fibroblasts. The cristae exhibited heterogeneous forms, ranging from tubular to lamellar (Fig. 2*D* and *SI Appendix*, Fig. S2*D*). The mean distance between neighboring crista junctions as measured on TEM sections from 10 independent fibroblasts was 100 ± 34 nm. This spacing is within the same range as seen for the distance of Mic60 clusters (*SI Appendix*, Fig. S2 *C* and *E*).

Dual-color STED images of mitochondria labeled for the outer membrane protein Tom22 and Mic60 demonstrated that the twisted arrangement of Mic60 can occur within non-constricted tubules, disproving the hypothesis that the twisted arrangements of Mic60 are limited to mitochondrial constriction sites (Fig. 2*E*). At the same time, these recordings demonstrate that the Mic60 band patterns are not a simple projection artifact, as such band patterns do not appear in the Tom22 channel. Tom22 is part of the translocase of the outer membrane (TOM) complex, which has been shown to interact with MICOS in yeast mitochondria (14, 16). However, discernible twisted band-like distribution patterns were found only for Mic60 clusters.

To further investigate the distribution of Mic60 in human cells, we immunolabeled human A-498 kidney carcinoma cells for Mic60 or Tom20 and recorded them with 3D STED nanoscopy (Fig. 2*F*, *SI Appendix*, Figs. S2*F* and S3, and Movie S2). After straightening the mitochondrial tubules in silico, the fluorescence signals of 1.5-μm-long mitochondrial segments were summed along the longitudinal mitochondrial axis. We analyzed 552 mitochondrial segments and found that in the majority of all segments, the Tom20 clusters were homogenously distributed without angular preference (Fig. 2*F* and *SI Appendix*, Fig. S3 *C*–*E*). The added fluorescence signals of segments decorated for Mic60 were clearly different (Fig. 2*F* and *SI Appendix*, Fig. S3). In approximately 17% of all segments, two clear opposing signals were visible (Fig. 2*F* and *SI Appendix*, Fig. S3*F*), corresponding to two parallel untwisted bands spanning the entire 1.5-μm segments. The remaining fluorescence signal distributions were fully in line with the view of Mic60 arranged in two twisted distribution bands, as the twisting is expected to smear out the summed fluorescence signal into rings with gaps, which was observed in 37% of all summed segments. This finding of twisted Mic60 bands is further supported by an animated view of consecutive virtual sections rectangular to the longitudinal axis of the mitochondria suggesting that the double-helical patterns originate from the twisting of the two distribution bands (Movie S2). Taken together, these data demonstrate that in different human cell types, Mic60 forms clusters that are enriched in opposing distribution bands, which can adopt a helical arrangement.

The Opposing Distribution Bands of Mic60 Are Largely Independent of the Cristae Morphology. We observed an enrichment of Mic60 in opposing distribution bands in yeast cells (Fig. 1 *A* and *B* and *SI Appendix*, Fig. S1*A*), primary HDFas (Fig. 2 *A* and *B* and *SI Appendix*, Fig. S2*A*), and human A-498 kidney carcinoma cells (Fig. 2*F*, and *SI Appendix*, Fig. S2*F*, and Movie S2). Under the growth conditions used here (i.e., logarithmically growing cells with galactose as carbon source), the cristae of the yeast cells generally did not fully span the interior of the mitochondria (Fig. 1 *C* and *D* and *SI Appendix*, Fig. S1 *E*–*G*), while the fibroblasts featured heterogeneous, tubular, or sheet-like cristae (Fig. 2*D* and *SI Appendix*, Fig. S2*D*). Thus, because the cristae do not necessarily span the matrix space, it appears likely that the opposing arrangement of Mic60 is not determined primarily by the cristae structure.

To further investigate the influence of cristae morphology on Mic60 distribution, we determined the distribution of Mic60 in mitochondria of Δ*mic10* yeast cells, which exhibit aberrant cristae. In Δ*mic10* mitochondria, the cristae membranes are largely detached from the inner boundary membrane, as the number of crista junctions is reduced (12, 15, 24, 25). Thus, if the cristae determine the localization of the Mic60 clusters, the distribution of these clusters would be predicted to be significantly changed in Δ*mic10* yeast cells.

Confocal recordings revealed bulbous mitochondria in ∼27% of the Δ*mic10* cells (compared with ∼4% in wild-type cells), but the majority of the cells still displayed tubular mitochondria as well (Fig. 3*A* and *SI Appendix*, Fig. S4*A*), which we used for further analysis. When recorded with STED nanoscopy, Mic60 clusters arranged in opposing distribution bands were visible in a large fraction of the mitochondrial tubules (Fig. 3*B*). The fraction of cells exhibiting at least one occurrence of twisted Mic60 distribution bands in a 2D STED image was slightly reduced to 30% in Δ*mic10* cells compared with 48% in wild-type cells; in addition, we observed longer parallel Mic60 arrangements without twisting in the Δ*mic10* cells (Fig. 3 *B* and *C*). Taken together, these data suggest that the arrangement of the Mic60 clusters at opposing sides of the mitochondria is largely independent of the cristae morphology.

Mic60-Interacting Proteins Also Localize in Distinct Clusters. The MICOS complex is composed of two subcomplexes: the Mic60 subcomplex, which encompasses Mic60 and Mic19, and the Mic10 subcomplex, which includes Mic10, Mic12, Mic26, and Mic27 in yeast (18, 26). To investigate whether the Mic10 subcomplexes also exhibit an ordered arrangement within mitochondria, we investigated the nanoscale distributions of Mic10 as well as of GFP-tagged Mic12 and Mic27 in yeast. As seen for Mic60, we found that these three proteins also form distinct clusters that are frequently arranged in patterns similar to those

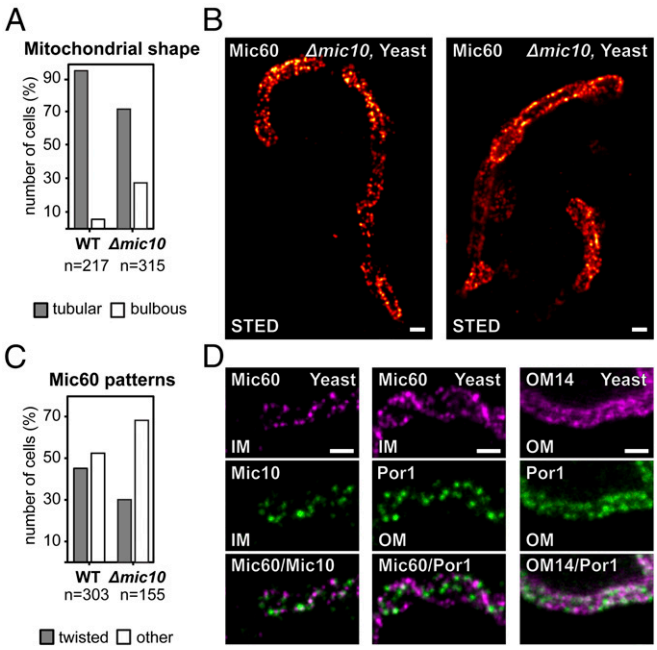

Fig. 3. Nanoscale distribution of yeast mitochondrial inner and outer membrane proteins. (*A*–*C*) Mitochondrial shape and Mic60-GFP distribution patterns in WT and *Δmic10* cells labeled with a GFP-specific antiserum. (*A*) Quantification of cells with tubular and bulbous mitochondria. (*B*) STED images of entire *Δmic10* yeast cells. (*C*) Quantification of twisted Mic60 distribution patterns in WT and *Δmic10* cells. (*D*) Dual-color STED nanoscopy of mitochondrial membrane proteins, as indicated. Mic10 and Por1 were labeled with specific antisera. Mic60 and OM14 were expressed from the respective native genomic loci as GFP fusion proteins and decorated with a GFP-specific antiserum. (Scale bars: 400 nm in *B* and *D*).

seen for Mic60 (Fig. 3*D* and *SI Appendix*, Fig. S4*B*). However, these patterns seemed to be less distinct than those that were recorded when the yeast cells were labeled for Mic60.

Because MICOS has been shown to engage in numerous physical interactions with proteins of the outer membrane in yeast (12–14, 16, 20), we next analyzed the submitochondrial distributions of several other of these interacting proteins, including OM14, a mitochondrial outer membrane receptor for cytosolic ribosomes; Tom20 and Tom40, subunits of the translocase of the outer membrane; and Por1, a voltage-dependent anion channel (mitochondrial porin). Intriguingly, we found that all these integral outer membrane proteins were enriched in clusters that appeared to be inhomogeneously distributed, suggesting an ordered arrangement of these proteins as well. However, the heterogeneity of the observed distribution patterns and the uncertainty of the degree of labeling due to the use of polyclonal antibodies with different binding affinities preclude a statistically robust quantitative analysis of the level of molecular interactions. Qualitatively, the distribution patterns of these proteins did not clearly match the helical pattern observed for Mic10 and Mic60 (Fig. 3*D* and *SI Appendix*, Fig. S4*C*). We conclude that the frequent qualitative observations of patterned mitochondrial membrane protein distributions, most notably in the case of Mic60, suggest a large-scale distributional organization of numerous proteins in the mitochondrial inner and outer membranes.

Discussion

This study shows that MICOS clusters in yeast and in different human cell lines are often distributed on opposing sides of a mitochondrion within distribution bands (Fig. 4). We find that these distribution bands can be twisted, resulting in a helical arrangement of the MICOS clusters (Figs. 1 *A* and *B* and 2*A*). Whereas we primarily observed such helical arrangements in the curved and highly dynamic networks of yeast mitochondria, extended untwisted arrangements are also visible in mammalian cells (Fig. 2 *A*–*C*). The latter has been reported previously (23), and here we demonstrate that an untwisted arrangement of the distribution bands can be contiguous with a helical arrangement.

In yeast mitochondria, our FIB-SEM data reveal short lamellar cristae that exhibit a twisted spatial organization. It was recently shown that the cristae of *Drosophila* indirect flight muscle mitochondria can also adopt a helical arrangement (27). Thus, such helical crista arrangements might be a common architectural feature across several cell types. Nevertheless, the occurrence of such twisted arrangements of cristae and crista junctions seems to be largely independent of the crista shape, as yeast mitochondria have relatively small and short lamellar cristae, while HDFa mitochondria have longer, tubular, or sheet-like cristae, and the helical cristae of *Drosophila* mitochondria are large lamellar structures. The wide spectrum of crista shapes associated with helical orientations argues against the idea of membrane physics being exclusively responsible for the intricate orientation of the cristae and the distribution of crista junctions.

Mic60 is an ancient protein (28, 29) that is enriched at crista junctions and has been demonstrated to bend membranes in vitro (11, 12, 23, 30, 31). The rather constant spacing of the crista junctions and localization of the Mic60 clusters in distribution bands that run along the length of the mitochondrial tubules argue for a connection of these clusters along the tubules. Indeed, several findings suggest that the Mic60 clusters are coupled not only along, but also across the mitochondrial tubules, independent of the cristae. First, in yeast cells, the short lamellar cristae do not span the mitochondrial tubules. However, an arrangement of protein clusters in opposing distributions bands is difficult to explain without proposing some kind of physical connection between the clusters across the mitochondrial tubules. Furthermore, the opposing distribution of Mic60 is maintained in *Δmic10* yeast cells that have aberrant cristae, also arguing for a physical connection of the Mic60 clusters across the mitochondrial tubules by a structure

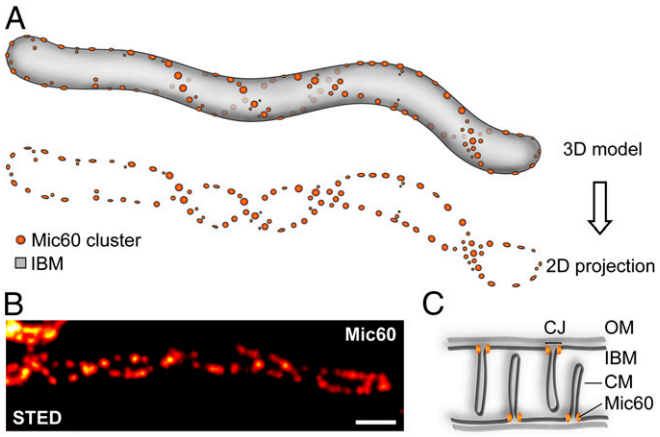

Fig. 4. Mic60 clusters are distributed in two opposing distribution bands of varying widths. (*A*) Cartoon showing the postulated distribution of Mic60 (Mic60 clusters are depicted as orange spheres) on a mitochondrial tubule. The inner boundary membrane is in gray. Note that the clusters are in opposing distribution bands of varying widths. The twisting of these bands varies, so that both helical and parallel arrangements are observed. Shown is a 3D cartoon (*Top*) and the projection of the Mic60 clusters into one plane. The latter corresponds to the situation in 2D STED nanoscopy, which, because of its diffraction-limited *z* resolution, projects the signals from an entire mitochondrion into one plane. (*B*) For comparison with the cartoon, a 2D STED recording of a moderately twisted Mic60 pattern (same image as in Fig. 2*B*) is shown. (*C*) Sketch of the mitochondrial membrane architecture. Mic60 is preferentially localized at the crista junctions (CJs). CM, cristae membrane; IBM, inner boundary membrane; OM, outer membrane. (Scale bar: 500 nm.)

within the mitochondrial membranes. Moreover, previous studies have shown that in yeast mitochondria devoid of crista membranes, the punctate labeling pattern of MICOS is not significantly changed (13, 18). Finally, our STED data suggest that in mammalian cells, the Mic60 clusters in one distribution band are spatially correlated with the clusters in the opposing band. Taken together, these findings suggest that the MICOS clusters are physically coupled along and across the mitochondrial tubules, presumably by proteins in the mitochondrial inner membrane.

We did not observe a continuous filamentous structure for any of the investigated MICOS subunits in yeast or mammalian cells. Thus, our data give rise to the intriguing idea that Mic60, and some of its interacting proteins, together form a large heterogeneous membrane-embedded structure that scaffolds the organelle.

In line with the idea of MICOS being a part of a scaffolding structure, deletions of the core subunits of the MICOS complex have drastic effects on the architecture of the mitochondrial inner membrane (11–13), as well as on the overall mitochondrial morphology (13, 32, 33). Mitochondria frequently undergo fusion and fission, thereby changing the network morphology (1, 3). Thus, any scaffolding structure would be expected to be flexible and heterogeneous. This fits with our finding that even the Mic60 localizations were highly variable, although they provided the clearest indication of the existence of a patterned distribution; therefore, the proposed structure (13) is expected to be flexible and heterogeneous. We predict that it is much less rigid than, for example, the periodic lattice of actin rings evenly spaced by spectrin tetramers found in the plasma membrane of neuronal axons and dendrites (34, 35).

Remarkably, yeast mitochondria devoid of both crista membranes and the MICOS complex have a tubular shape (18), suggesting that additional factors independent of MICOS contribute to the structural rigidity of the organelle. Indeed, MICOS interacts with a multitude of proteins in both mitochondrial membranes, which might be part of this structure (12, 13, 15–20). Thus, we suggest the existence of a structurally variable multiprotein structure in the mitochondrial inner membrane and potentially the outer membrane that scaffolds the organelle. We propose that this structure is the elusive mitoskeleton.

Materials and Methods

A detailed description of the methodology of this study, including the generation of yeast strains, immunofluorescent labeling of yeast cells, culturing of mammalian cell lines, 2D and 3D STED nanoscopy, statistical analysis, FIB-SEM of yeast cells, and TEM of HDFa cells, is provided in *SI Appendix, Materials and Methods*.

ACKNOWLEDGMENTS. We thank Anna Kremer and Saskia Lippens (VIB BioImaging Core) for acquisition of the FIB-SEM data; Peter Ilgen for help with 3D animations; Rita Schmitz-Salue and Gudrun Heim for excellent technical assistance; Peter Rehling for antisera specific to Tom40 and Mic10; Valentina Carannante for the A-498 cells and cell culture support; Hans Blom for STED support; Benedikt Westermann for the plasmid pVT100U-mt GFP; and Jaydev Jethwa for a careful reading of the manuscript. Infrastructure development support was provided by the Swedish Foundation for Strategic Research (RIF14-0091, to D.C.J.). This work was supported by the German Research Foundation-funded SFB1190 (project P01, to S.J.).

1. Bereiter-Hahn J, Vöth M (1994) Dynamics of mitochondria in living cells: Shape changes, dislocations, fusion, and fission of mitochondria. *Microsc Res Tech* 27:198–219.
2. Sesaki H, Jensen RE (1999) Division versus fusion: Dnm1p and Fzo1p antagonistically regulate mitochondrial shape. *J Cell Biol* 147:699–706.
3. Shaw JM, Nunnari J (2002) Mitochondrial dynamics and division in budding yeast. *Trends Cell Biol* 12:178–184.
4. Wasilewski M, Chojnacka K, Chacinska A (2017) Protein trafficking at the crossroads to mitochondria. *Biochim Biophys Acta Mol Cell Res* 1864:125–137.
5. Merkwirth C, Langer T (2008) Mitofusin 2 builds a bridge between ER and mitochondria. *Cell* 135:1165–1167.
6. Eisenberg-Bord M, Shai N, Schuldiner M, Bohnert M (2016) A tether is a tether is a tether: Tethering at membrane contact sites. *Dev Cell* 39:395–409.
7. Martijn J, Vosseberg J, Guy L, Offre P, Ettema TJG (2018) Deep mitochondrial origin outside the sampled alphaproteobacteria. *Nature* 557:101–105.
8. Pilhofer M, Jensen GJ (2013) The bacterial cytoskeleton: More than twisted filaments. *Curr Opin Cell Biol* 25:125–133.
9. Wagstaff J, Löwe J (2018) Prokaryotic cytoskeletons: Protein filaments organizing small cells. *Nat Rev Microbiol* 16:187–201.
10. Pfanner N, et al. (2014) Uniform nomenclature for the mitochondrial contact site and cristae organizing system. *J Cell Biol* 204:1083–1086.
11. Rabl R, et al. (2009) Formation of cristae and crista junctions in mitochondria depends on antagonism between Fcj1 and Su e/g. *J Cell Biol* 185:1047–1063.
12. Harner M, et al. (2011) The mitochondrial contact site complex, a determinant of mitochondrial architecture. *EMBO J* 30:4356–4370.
13. Hoppins S, et al. (2011) A mitochondrial-focused genetic interaction map reveals a scaffold-like complex required for inner membrane organization in mitochondria. *J Cell Biol* 195:323–340.
14. von der Malsburg K, et al. (2011) Dual role of mitofilin in mitochondrial membrane organization and protein biogenesis. *Dev Cell* 21:694–707.
15. Alkhaja AK, et al. (2012) MINOS1 is a conserved component of mitofilin complexes and required for mitochondrial function and cristae organization. *Mol Biol Cell* 23:247–257.
16. Bohnert M, et al. (2012) Role of mitochondrial inner membrane organizing system in protein biogenesis of the mitochondrial outer membrane. *Mol Biol Cell* 23:3948–3956.
17. Ott C, et al. (2012) Sam50 functions in mitochondrial intermembrane space bridging and biogenesis of respiratory complexes. *Mol Cell Biol* 32:1173–1188.
18. Friedman JR, Mourier A, Yamada J, McCaffery JM, Nunnari J (2015) MICOS coordinates with respiratory complexes and lipids to establish mitochondrial inner membrane architecture. *eLife* 4:e07739.
19. Harner ME, et al. (2016) An evidence-based hypothesis on the existence of two pathways of mitochondrial crista formation. *eLife* 5:e18853.
20. Rampelt H, Zerbes RM, van der Laan M, Pfanner N (2017) Role of the mitochondrial contact site and cristae organizing system in membrane architecture and dynamics. *Biochim Biophys Acta Mol Cell Res* 1864:737–746.
21. Huang B, Babcock H, Zhuang X (2010) Breaking the diffraction barrier: Super-resolution imaging of cells. *Cell* 143:1047–1058.
22. Sahl SJ, Hell SW, Jakobs S (2017) Fluorescence nanoscopy in cell biology. *Nat Rev Mol Cell Biol* 18:685–701.
23. Jans DC, et al. (2013) STED super-resolution microscopy reveals an array of MINOS clusters along human mitochondria. *Proc Natl Acad Sci USA* 110:8936–8941.
24. Barbot M, et al. (2015) Mic10 oligomerizes to bend mitochondrial inner membranes at cristae junctions. *Cell Metab* 21:756–763.
25. Bohnert M, et al. (2015) Central role of Mic10 in the mitochondrial contact site and cristae organizing system. *Cell Metab* 21:747–755.
26. Guarani V, et al. (2015) QIL1 is a novel mitochondrial protein required for MICOS complex stability and cristae morphology. *eLife* 4:e06265.
27. Jiang YF, et al. (2017) Electron tomographic analysis reveals ultrastructural features of mitochondrial cristae architecture which reflect energetic state and aging. *Sci Rep* 7: 45474.
28. Muñoz-Gómez SA, et al. (2015) Ancient homology of the mitochondrial contact site and cristae organizing system points to an endosymbiotic origin of mitochondrial cristae. *Curr Biol* 25:1489–1495.
29. Huynen MA, Mühlmeister M, Gotthardt K, Guerrero-Castillo S, Brandt U (2016) Evolution and structural organization of the mitochondrial contact site (MICOS) complex and the mitochondrial intermembrane space bridging (MIB) complex. *Biochim Biophys Acta* 1863:91–101.
30. Tarasenko D, et al. (2017) The MICOS component Mic60 displays a conserved membrane-bending activity that is necessary for normal cristae morphology. *J Cell Biol* 216:889–899.
31. Hessenberger M, et al. (2017) Regulated membrane remodeling by Mic60 controls formation of mitochondrial crista junctions. *Nat Commun* 8:15258.
32. John GB, et al. (2005) The mitochondrial inner membrane protein mitofilin controls cristae morphology. *Mol Biol Cell* 16:1543–1554.
33. Xie J, Marusich MF, Souda P, Whitelegge J, Capaldi RA (2007) The mitochondrial inner membrane protein mitofilin exists as a complex with SAM50, metaxins 1 and 2, coiled-coil-helix coiled-coil-helix domain-containing protein 3 and 6 and DnaJC11. *FEBS Lett* 581:3545–3549.
34. Xu K, Zhong G, Zhuang X (2013) Actin, spectrin, and associated proteins form a periodic cytoskeletal structure in axons. *Science* 339:452–456.
35. D'Este E, Kamin D, Göttfert F, El-Hady A, Hell SW (2015) STED nanoscopy reveals the ubiquity of subcortical cytoskeleton periodicity in living neurons. *Cell Rep* 10: 1246–1251.